

Landslides (2022) 19:1391–1404
 DOI 10.1007/s10346-022-01868-w
 Received: 24 October 2020
 Accepted: 18 February 2022
 Published online: 17 March 2022
 © Springer-Verlag GmbH Germany,
 part of Springer Nature 2022

Hengxing Lan¹ · Yixing Zhang · Renato Macciotta · Langping Li² ·
 Yuming Wu · Han Bao · Jianbing Peng



The role of discontinuities in the susceptibility, development, and runout of rock avalanches: a review

Abstract Rock avalanche is one of the most spectacular and catastrophic type of natural hazard phenomena. Those events typically start with a giant rock block or multiple blocks becoming detached from the rock slope, progressively fragmenting and transforming into rapidly moving cohesionless rock debris. Discontinuities are widely distributed in rock masses. Although research on rock avalanche phenomena is extensive, the role of discontinuities in different phases of rock avalanches, including the susceptibility, development, and runout phases, has not been systematically and comprehensively addressed, which has aroused a long-standing controversial issue. In this paper, the effects of discontinuities on the three phases of rock avalanches are systematically reviewed and discussed. The preexisting discontinuities influence not only the detachment of rock masses in the failure process but also their disintegration and propagation during runout. As a precursory factor, discontinuities control the kinematic feasibility of rock slope failure and the rock mass strength and thus control the susceptibility of the rock slope to failure as well as the size and spatial distribution of potential rock slope failure areas. During the development phase, the existing discontinuities will propagate and coalesce, increasing the slope fragmentation and decreasing the resistance to failure, and the kinematics of detachment evolve. It is worth noting that the evolution and failure phase would not happen, or just in moments in an earthquake-triggered events(s) or similar events. During runout, the control of discontinuities on rock avalanches is primarily reflected by shear and progressive fragmentation accompanied by heterogeneous distributions of stress and grain size, efficient energy transfer, and characteristic deposits. Nevertheless, dynamics of rock avalanches is complex, and controversial disputes remain; there is no straightforward conclusion. The inherent geology might play a dominant role in determining their strengthening or weakening effect in the various stages of rock avalanches. Several perspectives on future research are discussed, and approaches for focusing on the challenging research required to better our understanding of the role of discontinuities are suggested.

Keywords Discontinuity · Rock avalanche · Susceptibility · Failure development · Runout · Progressive fragmentation

Introduction

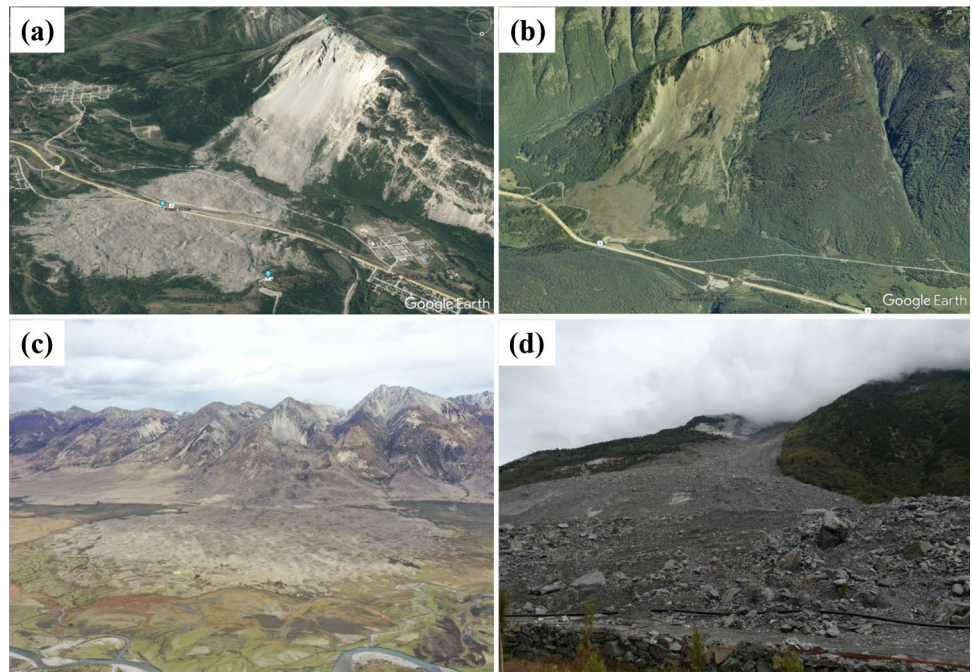
Rock avalanches ($\geq 0.5 \times 10^6 \text{ m}^3$) are initiated by the breakage of a large rock block detached from a near-vertical cliff face, followed by disaggregation into smaller rock blocks during the initial sliding/falling movement and further a transition into flow-like motion of fragmented rocks (Petley 2013; Strom 2021). Therefore, rock

avalanches generally develop from block slides to granular flows (Strom 2021). They have been documented and investigated since the nineteenth century and appear to be ubiquitous in mountainous regions (Petley 2013). Catastrophic examples include the Frank Slide (Cruden and Krahn 1973), the Hope Slide (Brideau et al. 2005), the Luanshibao rock avalanche (Wang et al. 2018), and the 24 June 2017 event that completely destroyed Xinmo village in China (Fan et al. 2017) (Fig. 1). Although most have been reported as isolated events, strong earthquakes in mountainous areas (e.g., the 1964 Alaska earthquake and the 2008 Wenchuan earthquake) can cause many large rock avalanches with severe consequences (Keefer 1984; Yin et al. 2009; Qi et al. 2011).

Rock avalanches are usually characterized by very high mobility and long runout potential. Their mobility is commonly quantified by the “apparent friction coefficient”, which is also called the “angle of reach” or “Fahrböschung”, as introduced by Heim (Corominas 1996; Lucas et al. 2014). Nevertheless, a better characterization of mobility other than the angle of reach has also been proposed (e.g., Strom et al. 2019). The reasons for the high mobility of rock avalanches, i.e., the apparent friction coefficients that are commonly lower than the friction coefficients of natural rock materials (Hsu 1975; Hutter et al. 1995), are still controversial open questions. As a consequence, research on rock avalanche phenomena is extensive, including evaluations of the failure mechanism of large rock slopes (e.g., Benko and Stead 1998; Seijmonsbergen et al. 2005; Crosta et al. 2014; Fan et al. 2017), physical experimentation to investigate parameters and mechanisms involved in rock avalanches (e.g., Dubovskoi et al. 2008; Manzella and Labiouse 2009; Paguican et al. 2014; Lin et al. 2020), and studies of the deposits to elucidate these phenomena (e.g., Crosta et al. 2006; Dunning 2006; Charrière et al. 2016; Dufresne et al. 2016).

Rock avalanche deposits typically present features such as multifacies, inverse grading and retention of rock mass characteristics (Hewitt 1999; Dufresne et al. 2016; Strom and Abdrakhmatov 2018; Schilirò et al. 2019), which are all associated with discontinuities within rock slopes. One common phenomenon in rock avalanche deposits is that rock mass disintegrates into numerous blocks with different sizes and shapes during runout processes. The role of those blocks in landslide movement has been gradually recognized by many researchers (e.g., Cagnoli and Romano 2012; Dufresne and Dunning 2017; Wu and Lan 2019, 2020; Lin et al. 2020). Those blocks are produced during progressive fragmentation and are largely determined by discontinuities. There has been a long-standing controversial issue regarding how discontinuities will affect the dynamics of rock avalanches. Some studies have suggested that disintegration following

Fig. 1 Views of the Frank Slide (a) (Google Earth image, 31 December, 2012), Hope Slide (b) (Google Earth image, 4 August 2004), Luanshibao rock avalanche (c) (photo from Hengxing Lan, 14 May 2020) and Xinmo landslide (d) (photo from Hengxing Lan, 5 September 2018)



discontinuities will increase the mobility of rock avalanches (e.g., Pollet and Schneider 2004), while others have argued that the existence of discontinuities may reduce runout because energy consumption will increase with the emergence of new surfaces (e.g., Locat et al. 2006; Crosta et al. 2007). It should be mentioned that the higher mobility of rock avalanches in high-latitude and high-elevation regions might be due to substrates with ice and snow. In addition, the slope inclination below the rock wall is also a constraining factor for the runout distance (e.g., Zhao et al. 2017). Nevertheless, discontinuities will play a role in rock avalanches.

There are several review papers about rock avalanches, focusing on, for example, basic characteristics and classification criteria (e.g., Strom 2021), body-substrate interactions (e.g., Dufresne 2014), and numerical simulations (Iverson and Ouyang 2015; McDougall 2017); however, none of them have specifically discussed discontinuities. Some papers have explicitly or implicitly suggested that discontinuities have effects on the runout of the center of the sliding mass (e.g., Lin et al. 2020); the final size, shape, and spatial distribution of large fragments (e.g., Zhao et al. 2018); and the formation and development of hummocks (e.g., Shea and de Vries 2008) of rock avalanches. The authors, however, are not aware of a major paper that systematically and comprehensively discussed the role of discontinuities in rock avalanches.

This paper presents a systematic review on the role of discontinuities in the susceptibility, development and, particularly, the runout of rock avalanches. First, some background considerations are briefly presented to introduce the reader to the discontinuities present at different scales and the different phases of a rock avalanche. Then, this paper discusses the control that discontinuities have on the susceptibility of large rock slopes to failure and development during the initiation of slope collapse. This is followed by a description and discussion on the role of discontinuities during the runout phase. Finally, we present our perspectives for future research.

Background information and initial considerations

Scale of discontinuities

Discontinuities within a rock slope can include faults, bedding planes, joints, and cleavage at the macroscale and microscale (Palmström 2001; Bao et al. 2019, 2020) (Fig. 2). A size-based classification of discontinuities is presented in Fig. 3. Their characteristics can be altered by various processes, including changes in the stress regime (e.g., unloading in response to river or glacial erosion and loading in response to earthquakes) and weathering (e.g., freeze-thaw cycling). Macroscale discontinuities can be observed unaided, but some discontinuities and defects (Fig. 2) in “intact” material can only be seen with the help of specialized apparatuses (e.g., electron microscopes) (Lan et al. 2019).

Phases of rock avalanches

In this paper, three different phases of rock avalanches are defined.

1. An initial phase, during which rock slopes undergo processes that lead to an increased susceptibility to failure and processes that weaken the slope materials (e.g., tectonic activity and weathering)
2. A failure development phase, during which joint and fracture networks develop more tensile cracks and the deformation accelerates, which leads to at least part of the rock slope mass moving along the basal failure plane
3. A rapid movement phase, during which intact blocks fragment into numerous blocks with different sizes and shapes

These three phases are summarized and presented by a simple sketch of the evolution of the famous Frank Slide in Alberta,

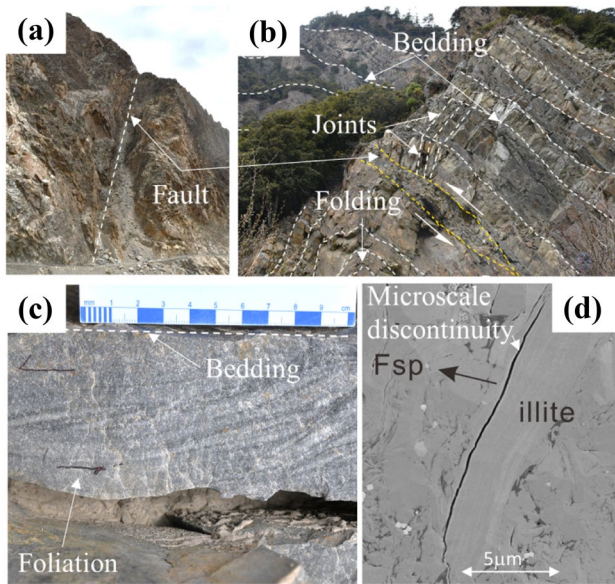


Fig. 2 Discontinuities at different scales within a slope-forming rock mass. Fault dividing granite and slate in southeastern Tibetan Plateau, China (a); bedding, cross-bedding joints, fault, and accompanying folding within sedimentary formations in Nyingchi, China (b); bedding and foliation in a sample of metamorphism gneiss in Nyingchi, China (c); and microscale cracks in the Longmaxi Shale from Sichuan Province, China (d). Photos from Hengxing Lan

Canada (Fig. 4). In this sketch, changes in the lithology in the South Peak of Turtle Mountain are illustrated by changes in shading and correspond to those described by Cruden and Krahn (1973); major tectonic faults are identified with solid black lines; discontinuities originating from tectonic uplift and rock mass shearing are identified with dashed black lines; bedding and discontinuities associated with bedding are identified with solid and dashed gray lines, respectively; the main sliding plane is identified with the solid red line; and the failed mass is identified with dotted black lines (Fig. 4). Although the origin of the Frank Slide was possibly accompanied by anthropogenic factors, it still presents three phases that are applicable for illustrating general cases. Another reason for choosing the Frank Slide for illustration is that it has been intensively

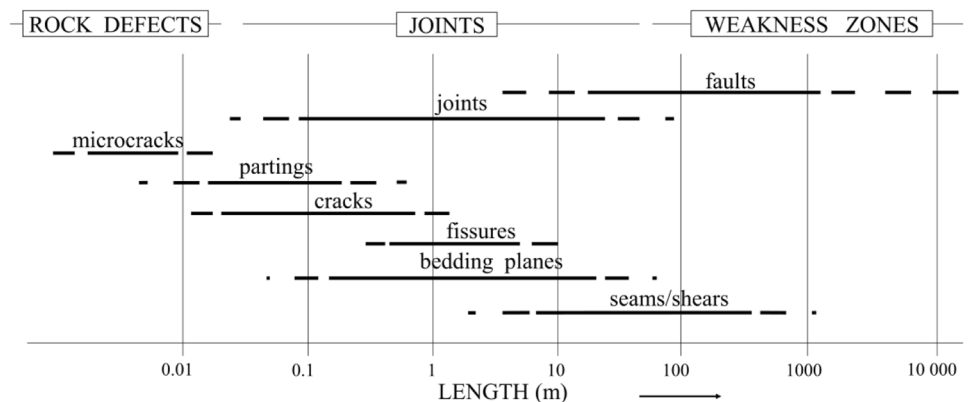
and comprehensively investigated (e.g., Cruden and Krahn 1973; Pedrazzini et al. 2012; Charrière et al. 2016).

It must be mentioned that for rock avalanches triggered by earthquakes, the second phase will not happen, or strictly speaking will occur in moments. Nevertheless, the definition of the three phases can involve both earthquake-triggered rock avalanches and cases that evolve to failure over time and therefore are necessary. Earthquake-triggered rock avalanches can be discussed in the context of phases 1 and 3, ignoring phase 2.

During the initial phase, the rock mass and discontinuity characteristics define the slope susceptibility to failure. Large slopes can develop various features, such as giant and cohesionless joints, intense fracturing, and slickensides. Most of these characteristics are inherited from tectonic deformations and sedimentation, and large-scale discontinuities might also be formed in rock slopes during seismic activities. Further weathering and deformation can lead to an increased susceptibility to failure through the coalescence of discontinuities and cohesion loss within the rock mass (Lan et al. 2003, 2004, 2010). This initial phase is commonly characterized by extremely slow deformation with poorly developed discontinuities in the rock mass, and the trend of deformation velocity is illustrated in Phase 1 in Fig. 5. Figure 4a shows a simple sketch of the initial phase for the Frank Slide. The initial phase in Fig. 4a corresponds to the stage in which discontinuities slowly develop a basal sliding zone.

The development of a rock slope failure (second phase of continued activity leading to slope collapse) has been the subject of a considerable amount of research. Field studies, numerical analyses, and monitoring results have shown that this stage is characterized by one or a combination of substantial deformation, accelerating and decelerating periods, and rock mass dilation. In this phase, certain features, such as breakaway scarps and tensile cracks, which are commonly controlled by discontinuities, are observed (Fig. 4b). This phase can be reached after further weathering and disaggregation of the rock mass, typically through coalescence of discontinuities and/or the formation of through-going shear zones. During this phase, discontinuity-bounded blocks with larger scales appear in the rock slope, and an increase in the deformation velocity is commonly observed (Fig. 5). In some cases, reactivation or long-term slow motion can still occur within the remaining intact rock mass behind (above) the detachment zone after failure.

Fig. 3 Main types of discontinuities and their average lengths (Palmström 2001)



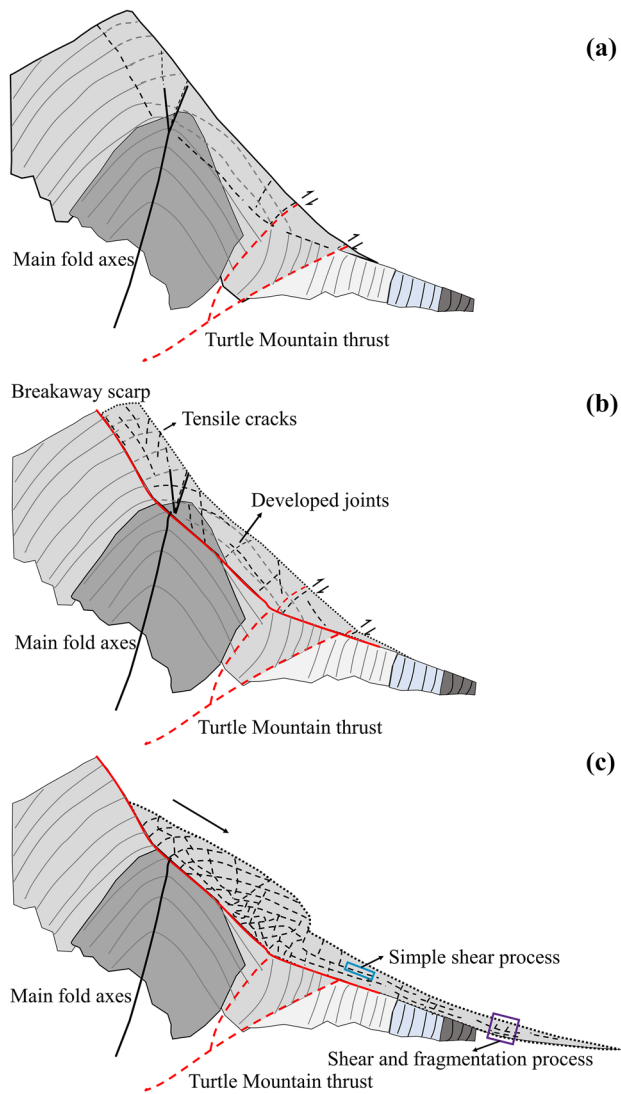


Fig. 4 A sketch of the initial (a), development (b), and movement (c) phases of a representative rock avalanche. The purple rectangle indicates one of the positions where “shear and fragmentation processes” occur within the moving rock mass, which is described in more detail in Fig. 8. The blue rectangle indicates one of the positions where “simple shear processes” occur within the moving rock mass, which is described in more detail in Fig. 9. Not to scale. Figure modified after Cruden and Krahn (1973) and Charrière et al. (2016)

The third phase, exhibiting extremely rapid movement and accumulation, is the most destructive and catastrophic (Fig. 4c). Large rock masses detach from high elevations and rapidly travel a few kilometers toward valley floors in a matter of minutes, or in some cases across valleys to the opposite slope. Weak discontinuities could cause stress and shear concentrations, forming numerous blocks with different sizes and shapes. Notably, the size and distribution of these blocks are not disorderly but regular (see “Observations from realistic field cases”). The velocity of the sliding mass is extremely fast (Fig. 5) and occurs as a coherent or at least partially coherent body due to the flow-like materials (numerous blocks).

(a)

(b)

(c)

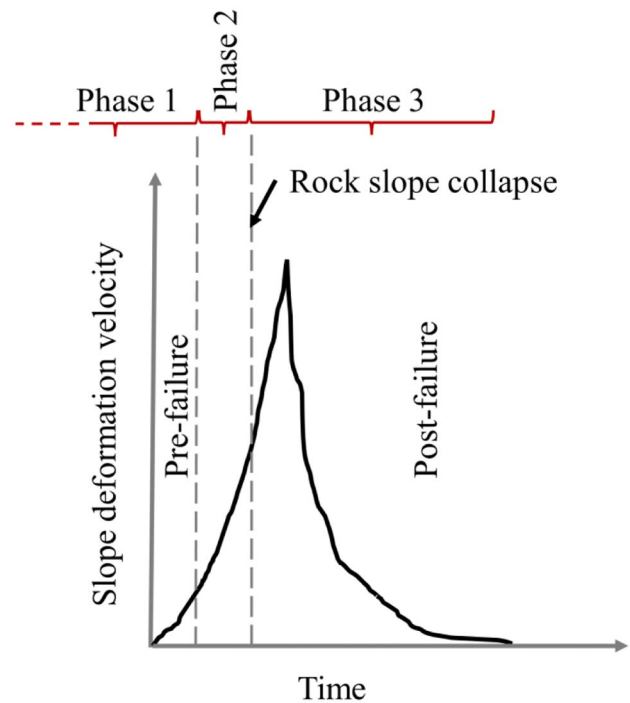


Fig. 5 Conceptualized deformation velocities for each of the phases of a rock avalanche in the context of landslide velocities. Figure modified after Leroueil (2001)

The above description of the three phases of rock avalanches suggests that the role of discontinuities in rock avalanches is non-negligible.

Role of discontinuities in the susceptibility and development of rock slope failures

Discontinuities and the susceptibility of rock slopes to failure

The tectonic history of an area can provide the trigger for large earthquakes and landslides (Barth 2014). Seismic activity can cause entire rock slopes, especially those along active faults, to disaggregate into several giant cohesionless rock blocks. In addition, faulting and seismicity lead to strong loading and folding and cause the formation of structural planes with different scales in rock masses (Kim et al. 2004). Those areas might be prone to be source areas of rock avalanches. Macro-structural planes provide preliminary weaknesses that can become part of primary sliding planes (Weidinger et al. 1996; Schramm et al. 1998). Under these conditions, an initial large fissure on the slope produced by earthquake loading can lead to the occurrence of rock slope failure and subsequent rock avalanche (Strom 2006).

It has been widely recognized that the spatial distribution of rock avalanches triggered by large earthquakes is clustered along active faults (Strom and Korup 2006; Weidinger 2006). Faulting and seismicity leading to a region prone to large landslides can be observed in the Wenchuan earthquake (e.g., Yin et al. 2009; Dai et al. 2011; Qi et al. 2011); rock avalanches triggered by this event are found to cluster along the faults with an average distance of 2.5 km

away (Fig. 6). In addition, source areas and transition areas of rock avalanches are intersected by active faults in many case studies (e.g., Xu et al. 2012; Wang et al. 2018).

Large-scale discontinuities provide kinematic contexts, such as detachable and cohesionless rock blocks. Small-scale discontinuities can affect the overall strength of rock mass. With time, increased damage to rock slopes due to internal and external factors (e.g., weathering, internal deformations, human activities, seismic loading, and river undercutting) will increase their susceptibility to initial slope failure (Li et al. 2017; Donati et al. 2020).

Discontinuities and the development of rock slope failures

Continued slope deformation, leading to the coalescence of discontinuities and weakening of the rock mass, increases the susceptibility of the rock slope to failure, resulting in the transition to a phase where deformation accelerates and failure develops (Lan et al. 2005, 2010; Donati et al. 2020). Therefore, there are many weathered and/or oxidized joint planes within the rock mass in the rock avalanche source area. The opening discontinuities allow for runoff water to infiltrate the rock mass and potentially trigger slope collapse (Catane et al. 2008; Xu et al. 2012). For example, it is found that the initiation zone of the 2000 Yigong landslide had five joint sets that, in combination with micro-crack propagation and pore water

pressure changes in the rock mass under the effect of freeze–thaw cycling, led to slope collapse (Zhou et al. 2016).

During the deformation phase, the rock mass response was mainly controlled by faults and joint networks. Oppikofer et al. (2008) used sequential terrestrial laser scanning point clouds to quantify the deformation of a rock slope and found that pre-failure deformations were controlled by the various discontinuities present in the slope. Severin et al. (2014) used ground-based radar and observed that the movement, block separation, and yielding of a rock mass in an open pit slope were defined by structures in the rock. In addition, tensile cracks and scarps can be clearly seen in field surveys or satellite imagery at the trailing edge. For instance, in 2017, a rock avalanche buried Xinmo village in Maoxian County, Sichuan Province, China; several clear head scarps were observed by optical satellite images collected during different phases of deformation (Fan et al. 2017). These scarps form along weak planes within the intact rock body. When tensile stresses are large enough, the weak plane detaches, becoming a daylighting discontinuity, and more movable large rock blocks detach from the intact source rock.

Before a large rock mass dynamically disintegrates, the failure process usually involves an initial unloading stage as rock falls or small rockslides or collapses (Crosta et al. 2007; Hungr et al. 2014). This trend has been witnessed for many non-seismic-induced rock avalanches (e.g., Crosta et al. 2007; Catane et al. 2008; Yin et al. 2011;

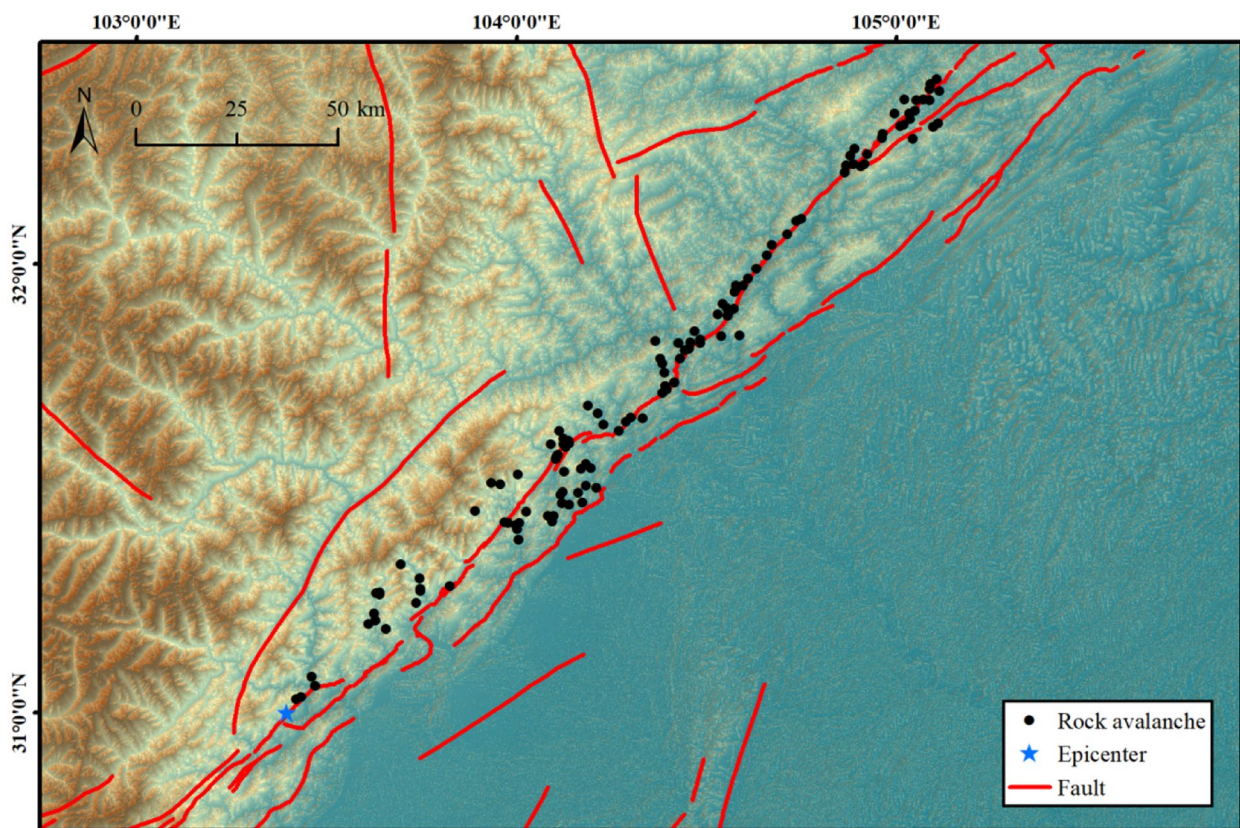


Fig. 6 Locations of rock avalanches in the Wenchuan earthquake-influenced area. The rock avalanche data are from Qi et al. (2011) and Xu et al. (2011). Rock avalanches with areas smaller than 100,000 m²

are not shown. The shaded relief map was created from the Shuttle Radar Topography Mission digital elevation model (<https://earthexplorer.usgs.gov/>)

Xu et al. 2012; Aaron and Hungr 2016). For instance, during field investigations performed a few days before the occurrence of the Jiweishan rockslide–rock avalanche, falls of thousands of cubic meters were generated (Yin et al. 2011). This phenomenon suggests that rock had detached and become unstable because of the coalescence and formation of discontinuities.

The development of the base sliding surface and the bedding plane inclination are both crucial for triggering collapse and have a significant impact on the failure volume (Dai et al. 2011; Vick et al. 2020a, b). The Xinmo village rock avalanche, which occurred in Mao County, Sichuan Province, China (24 June 2017), is a typical case of rock slope failure along dominant joints and bedding planes. It is clear that the rock mass slid along a bedding plane (attitude N80°W/SW $\angle 47^\circ$) (Fan et al. 2017; Fig. 7). Slickensides and bedding planes are commonly observed along the scarp and sliding planes after failure. Similar failure surfaces provided the conditions for the Frank Slide (e.g., Locat et al. 2003) and others (e.g., Aaron and Hungr 2016). Therefore, the coalescence of preexisting discontinuities and accompanying discontinuity-bounded blocks can trigger the failure of the rock slope.

Role of discontinuities in the runout of rock avalanches

Mechanisms for discontinuities affecting runout

The high mobility of rock avalanches cannot be ascribed to simply the lower friction coefficient of the basal layer without considering the changes that occur inside the sliding mass as it flows (Abele 1994; Campbell et al. 1995; Clavero et al. 2002; Strom 2015; Johnson et al. 2016; Zhang et al. 2016; Zhang and McSaveney 2017). Given the assumption that the sliding body is moving due to a lower frictional resistance along the sliding surface, the entire sliding body should accelerate, which the rheological behavior changes observed in the field do not support (Strom 2015). Internal friction in the sliding mass should be considered to unravel the long runout of rock avalanches.

Physical experiments have revealed that the high shear rates of granular particles could reduce the internal friction (e.g., Bagnold



Fig. 7 Bedding planes observed at the scarp and failure surface of the Xinmo village rock avalanche in 2017. Photo from Hengxing Lan, 5 September 2018

1954), cause higher damage (Zhang and McSaveney 2017), and facilitate high mobility (Lin et al. 2020). Intensive shear and fragmentation processes are common in the movement phase of rock avalanches. Those processes could be described through a widely accepted simplified facies model (Fig. 8) (e.g., Pollet and Schneider 2004; Crosta et al. 2007; Davies and McSaveney 2009; Dunning and Armitage 2011; Dufresne et al. 2016; Strom and Abdrakhmatov 2018; Wang et al. 2018) and appear along the preexisting discontinuities or weaknesses in lithologic units (Pollet and Schneider 2004; Dunning 2006; Crosta et al. 2007; Pedrazzini et al. 2013; Weidinger et al. 2014). Shear zones (subparallel, subvertical or horizontal) are common both within the body and at the base of rock avalanche deposits (e.g., Schramm et al. 1998; Charrière et al. 2016; Dufresne et al. 2016; Wang et al. 2019). A lack of weak planes will limit the formation of shear zones in the moving body and at the base of the rock avalanche (Dufresne et al. 2016). In addition, slab-on-slab shearing and shear zones form, as illustrated in Fig. 9, according to numerous field surveys (e.g., Pollet and Schneider 2004; Strom 2006; Charrière et al. 2016; Wang et al. 2019). Weak layers (slab-on-slab) within the rock make laminar flow possible, and the deposits present pseudostratified bodies without any mixing (Strom 2015).

Therefore, shear and fragmentation processes dominated by discontinuities reduce the internal friction and further facilitate the long runout of the sliding mass. It has been suggested that joints

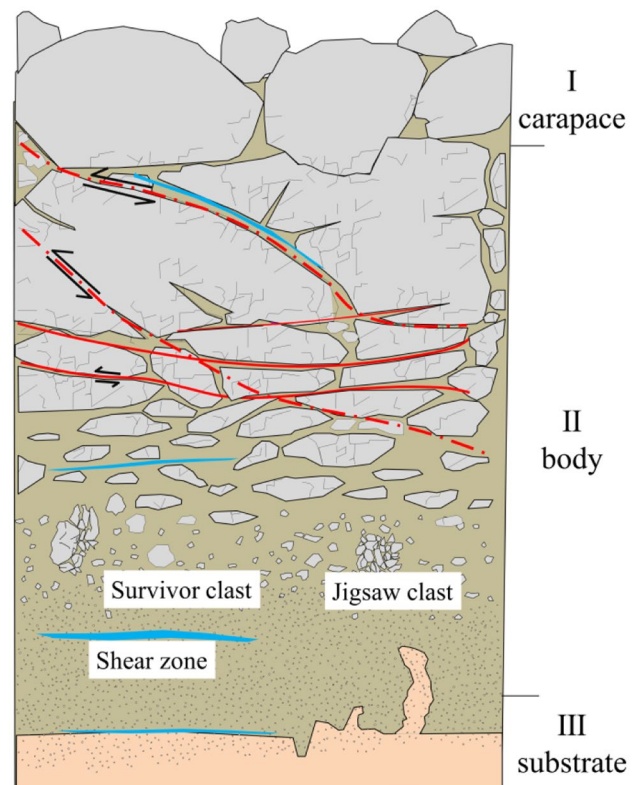
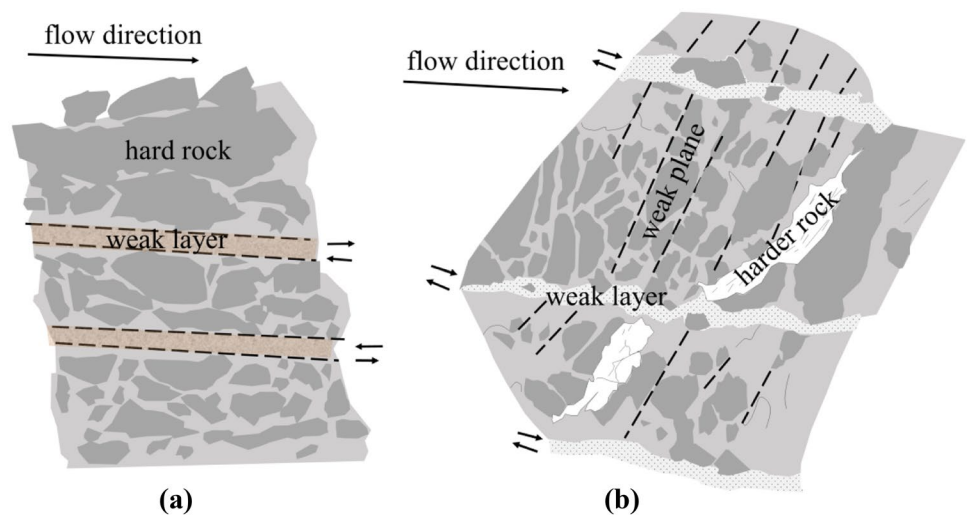


Fig. 8 Fragmented rock in the facies model of rock avalanches. The red solid lines denote subparallel shear zones. The dashed lines denote other shear zones along weak layers formed by impact. The blue areas denote surviving shear zones. Not to scale. Figure modified after Weidinger et al. (2014) and Dufresne et al. (2016)

Fig. 9 Sketches showing rock mass movement affected by preexisting weak layers and discontinuities. The dashed lines denote the weak planes. The gray blocks denote fragmented hard rock, and the white blocks denote harder rock. Movements parallel to weak layers are shown in both **a** and **b**. Not to scale. Figure modified from Pollet and Schneider (2004)



can lead to a reduction in frictional resistance (Corominas 1996), a reduction in shear strength by approximately 30% (Zhang et al. 2018b), or a very low residual strength (no cohesion with internal frictional angle ranging from 10° to 25°) along rupture surfaces (Wang et al. 2017), which can allow the moving rock mass to achieve longer runouts than expected.

In addition, the finest fraction of rock avalanche deposits can occupy over 90% of the fragment surface area, and the diameter of those materials is usually less than 1 μm (Davies et al. 2020). Therefore, the energy dissipation consumed in this part cannot be ignored during rock avalanche movement. According to the assumption of the Griffith theory of failure on the micron scale, in which most of the energy is utilized in creating a new rock surface, not enough energy is dissipated by fracture formation and frictional resistance during the rock avalanche movement phase (Davies et al. 2020). Therefore, Davies et al. (2020) showed that most of the energy is not consumed during microscopic brittle failure by enlarging suitably oriented defects but is consumed by efficient energy dissipation in the form of elastic body-wave energy disaggregating materials formed during shearing and fragmentation, and previously cracked grains on the microscopic scale play a key role in efficient energy dissipation. On the macroscopic scale, heterogeneous blocks and pressure distributions lead to larger deformations than those due to homogeneous blocks and pressure distributions (Lan et al. 2010). Therefore, microscopic and macroscopic discontinuities both contribute to increasing the runout width and length of rock avalanches.

Observations from realistic field cases

Observations from realistic field cases have also explicitly or implicitly suggested that discontinuities have effects on the runout of the sliding mass. In the long-runout Luanshibao rock avalanche, discontinuities are widely found in the scarp and deposit carapace (Fig. 10), suggesting that discontinuities may play a non-negligible role in both the failure and movement phases. Surveys of field cases were performed either in detail on individual cases or in a statistical manner based on many cases.

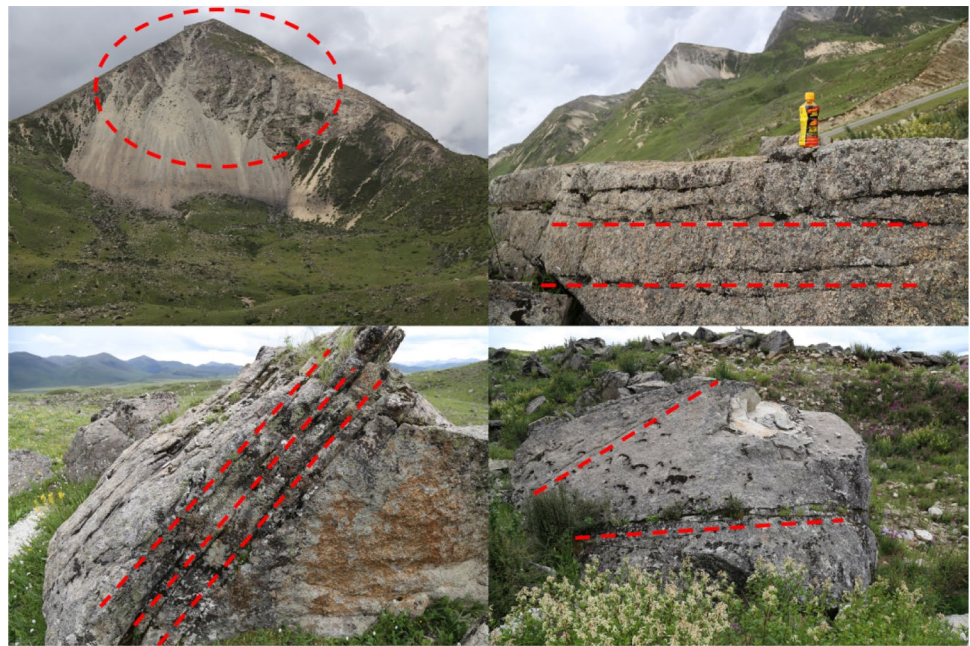
Detailed surveys of individual field cases commonly attempt to relate the characteristics of blocks in deposits to discontinuities in the source area. Numerous heterogeneous blocks will be produced during the movement phase of rock avalanches. Charrière et al. (2016) performed a quantitative analysis of the block volumes in the deposit carapace of the Frank Slide and found that the discontinuities in the source area controlled the block size distribution in the deposit carapace, and the block volumes in both areas could be described by a lognormal distribution. The discontinuities in the source area of the Frank Slide were also very well developed according to previous research (Charrière et al. 2016). Therefore, the block size distribution of the carapace can partly reflect and represent the characteristics of discontinuities in the source area, which has also been recognized by other studies (Kent 1966; Weidinger et al. 2014; Charrière et al. 2016; Wang et al. 2019).

Interesting patterns of the heterogeneous distribution of deposit block size have been revealed by quantitative statistics (Fig. 11) (e.g., Zhang et al. 2016; Wang et al. 2020). The block size is more heterogeneous in the initial part of the deposition area, and it gets smaller and becomes more homogeneous toward the distal part (Fig. 11), which has also been recognized by other studies (Charrière et al. 2016). The Frank Slide, which has a heterogeneous block size distribution across the deposition area (Charrière et al. (2016), propagated far away from the source. Lan et al. (2010) studied the micromechanical extensile behavior of rock and revealed that micro-tensile cracks produced by grain-scale heterogeneous block size distribution can accumulate and develop into mesoscopic tensile cracks and macro-fractures, facilitating the development and propagation of macro-cracks. Compared with homogeneous materials, heterogeneous blocks can induce larger deformations and transfer kinematic energy more efficiently (Lan et al. 2010). Discontinuities in the source area affect the block size distribution (Dunning 2006; Dunning and Armitage 2011), stress distribution (Aaron and Hungr 2016; Dufresne et al. 2016), and runout distance (Sun et al. 2021).

Implications of numerical and physical experiments

Multiple studies have been dedicated to simulating and calibrating the long runout lengths of rock avalanches that have occurred.

Fig. 10 Widely distributed discontinuity sets in the rock mass of the scarp and large blocks (only some are shown in the figure) in the deposit carapace of the Luanshibao rock avalanche. Photos from Hengxing Lan, 14 July 2020



Numerical models are extensive, but there are no universal constitutive laws that can be adopted (Pastor and Crosta 2012). To date, various numerical models have been developed and applied to simulate many rock avalanches and can be generally grouped into two categories: continuum models and discontinuum models (Table 1).

Continuum models usually use depth-averaged shallow flow equations (McDougall 2017). The movement of blocks in the sliding body is ignored when adopting depth-averaged shallow flow equations, and most are used to predict travel distance, deposit depth, and runout time (Wu and Lan 2019). Although a considerable amount of information is gained through the above approach, a next step to achieve more comprehensive predictions requires considering other features of the deposits (Thompson et al. 2010; Dunning and Armitage 2011; Strom 2015; Dufresne et al. 2016). In addition, solving for large deformations remains a challenge in continuum modeling. The disaggregation stage implies brittle behavior of the initially intact rock mass, leading to fragmentation. To solve for the rock characteristics that would arise from behavior, discontinuity development would need to be considered in the simulated model. Modeling large block surfacing and movement in marginal areas of the deposit during runout (Sosio et al.

2008; Aaron and Hungr 2016) are also challenging for continuum approaches. Another disadvantage of continuum approaches is associated with the assumption that a mass flow is a homogenous material, even when different lithologies are involved (Margielewski 2006; Crosta et al. 2007).

Discontinuum models have the advantage of integrating complex features. For example, different lithologies of the rock mass can be represented in discontinuum models, and propagation of discontinuity and brittle behavior can be modeled (Thompson et al. 2010; Lan et al. 2019). The distinct element method (DEM) (Cundall and Strack 1979) has been widely used to reproduce long-runout rock avalanches (Taboada and Estrada 2009; Boon et al. 2015; Zhao et al. 2016, 2017; Wang et al. 2017). The DEM can reproduce more details of certain phenomena, such as reverse grading, the decrease in block size with increasing travel distance, and the retention of the characteristics of the source area. In particle flow code (PFC) modeling of the Jiweishan rock avalanche, shear-induced fragmentation and characteristics of deposits were reproduced by considering bedding planes and joints in the source area rock mass (Zhang et al. 2019). Using discontinuous deformation analysis (DDA) modeling, Wang et al. (2021) found

Fig. 11 Block size distributions at different locations in the deposition area along the central axis of the rock avalanche. Each column in the bar graph indicates a location where block size data are collected. Distance is measured from the headscarp of landslide. Data in **a** and **b** are from Zhang et al. (2016) and Wang et al. (2020), respectively

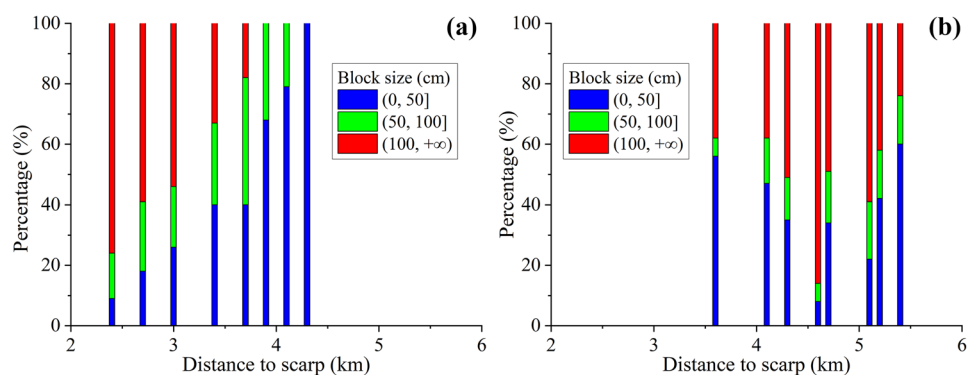


Table 1 Major numerical landslide runout models

Model	Type	Y/N ^a	Reference
DAN3D	Continuum	N	Aaron and Hungr (2016)
PFC	Discontinuum	Y	Thompson et al. (2010); Zhang et al. (2019)
MassFlow	Continuum	N	Ouyang et al. (2017)
MatDEM	Discontinuum	Y	Scaringi et al. (2018)
MassMov2D	Continuum	N	Beguería et al. (2009)
LS-RAPID	Continuum	N	Sassa et al. (2010)
r.avaflow	Continuum	N	Mergili et al. (2012, 2017)
LA	Hybrid	Y	Wu and Lan (2019)
DDA	Discontinuum	Y	Zhang et al. (2018a); Do and Wu (2020)

^aY: some properties of discontinuities can be considered in numerical modeling

that the degradation in the shear strength of rock masses controlled by joints significantly contributed to the long runout distance and high velocity of the Donghekou rock avalanche. In addition, by considering the block size distribution determined by the source area structures, the velocity of the sliding mass and the deposit morphology were reasonably reproduced for the Xinmo landslide (Wu and Lan 2019). These studies provide promising results and inexplicitly indicate the importance of discontinuities for shear fragmentation, block size distribution, and runout; however, more reliable predictions of runout still require additional efforts, e.g., more precise representations of the characteristics of source area discontinuities.

Physical experiments play a significant role in gaining a better understanding of the propagation mechanisms and factors influencing the velocity and deposit characteristics of rock avalanches (Manzella and Labiouse 2009). Due to the volume effect of rock avalanches or the difficulty in matching the scaling laws, many physical experiments have focused on a few limited factors (e.g., fragmentation, basal substrate, and topography). The results of some physical experiments have revealed the discontinuity effect on rock avalanches. Manzella and Labiouse (2009) showed experimental evidence that the sliding mass will travel longer by involving modeled discontinuity sets. Lin et al. (2020) performed groups of experiments with different configurations of analog blocks and suggested that shearing concentration or the slab-on-slab form of motion inside the sliding mass may facilitate the high mobility of rockslides and rock avalanches. Paguican et al. (2014) simulated the formation of hummocks using different material layers based on scaled analog models and found that preexisting discontinuities affect the kinematics and dynamics of hummocks through shear processes. Similar other scaled analog experiments on the formation and evolution of hummocks have also been performed (e.g., Shea and de Vries 2008). Those analog models show that different lithologies are key in the formation of hummocky topography in rock avalanche deposits and create conditions for shear and fragmentation processes. The constraints of discontinuities on shear fragmentation and block size have also been recognized by many other physical experiments considering the rock mass structure (e.g., Bowman et al. 2012; Haug et al. 2021; Lin et al. 2021).

Perspectives on further research

A considerable amount of research has been completed to understand the role of discontinuities at the macroscale and microscale in the susceptibility of large rock slopes to failure, slope failure mechanisms, and progressive slope fragmentation. Field observations, physical simulations, and recent numerical models suggest that the role of structure is also important during the runout of large rock avalanches; however, this has not been researched in depth. The aim of this section is to provide some perspectives on the future fieldwork, numerical modeling, and physical experiments required to gain a better understanding of the role of discontinuities in the runout of large rock avalanches.

Complementing evidence from field cases

The characteristics of field rock avalanche cases are commonly described qualitatively or semi-quantitatively, accompanied by few quantitative measurements (e.g., Legros 2002; Guo et al. 2014; Li et al. 2014, 2016; Lucas et al. 2014; Zhan et al. 2017; Mitchell et al. 2020; Strom et al. 2019). Statistical analysis based on many field cases commonly focuses on the constraints of volume and topography on the runout (e.g., Zhan et al. 2017; Strom et al. 2019) and seldom considers discontinuities. With the help of remote sensing technology (e.g., terrestrial laser scanning and unmanned aerial vehicle survey), some researchers have studied the relationship between the structural plane of the source area and the deposit carapace block (e.g., Charrière et al. 2016) and found that the source area's fracturing exhibits a primary control on the block size distribution of the surficial deposits based on statistical analysis. It is recommended, based on more field cases and sample locations, to perform statistical analysis to reveal the relationship between the characteristics of discontinuities in the source area (e.g., density, length, aperture, and dip angle) and the runout of rock avalanches. It is also suggested to focus on typical unconfined cases, such as the Frank Slide (Charrière et al. 2016), Luanshibao rock avalanche (Wang et al. 2018), and Tagarma rock avalanche (Wang et al. 2020), for which more ideal exposure conditions in the source areas and deposits are expected. In addition, a comparison between the runout of rock avalanches and the characteristics of rock

discontinuities should be performed when the other factors are similar. Therefore, a more detailed categorization of datasets based on influencing factors will reduce the scattering in observations, making the resulting correlations between rock mass properties and avalanche characteristics more revelatory (e.g., Nicoletti and Sorriso-Valvo 1991; Corominas 1996; Guo et al. 2014; Mitchell et al. 2020; Strom et al. 2019).

Advancing numerical and physical experiments

The critical role of pre-failure structures in the shear and fragmentation processes of rock avalanches has been demonstrated by various numerical (discontinuum) and physical simulations (e.g., Zhao et al. 2018; Lin et al. 2020; Wang et al. 2021). However, some simulations, such as DEC and DDA (see Table 1), do not consider the emergence and evolution of new discontinuities during fragmentation, especially those formed due to coalescence of smaller joints and breakage along weak planes, leading to real fragmentation processes that cannot be simulated. Some simulations, such as PFC and MatDEM (see Table 1), can consider complex fragmentation processes but are limited by the number of particles. Increasing the ability of the DEM to simulate a large number of particles and represent realistic discontinuities in the failure mass is still a major challenge. Wang et al. (2021) found that different discontinuities yield almost identical runout distances, but the same material and simple configurations of discontinuities were used in different simulations, and realistic discontinuities, including different weak layers, were not considered. In addition, it is also significant to quantitatively characterize the complex discontinuities in the failure and sliding rock mass using various parameters, such as number, length, space, and dip, which could be obtained based on geographic information science technology. The relationship between those parameters describing discontinuities and the runout of rock avalanches will be indicative. In numerical simulations, the evolution of those parameters during the sliding processes could be revealed. However, there are only a few studies that have investigated the quantitative relationship between discontinuities and runout. For example, the correlation between the dominant joint dip angle and the landslide mobility index (H/L) has been studied by numerical simulations (Sun et al. 2021); however, only the control of joint dip on the failure process of landslides has been considered.

In addition, simulations of the shear and fragmentation processes and the accompanying development of new discontinuities are still challenging because of the difficulties in obtaining and representing the information of complex discontinuities. Difficulties in obtaining pre-failure discontinuity information in the source area can be overcome through novel techniques, such as laser scanning (Jaboyedoff et al. 2007) or photogrammetry at the back scarp of the rock slope. Macciotta and Derek (2015) found a direct way to use the block size distribution at the source of a rock fall calculated through photogrammetric techniques to develop a discrete fracture network with the surveyed rock block sizes. Mapped discontinuities can be used to calculate block sizes in the rock mass at the source of rock avalanches through several methods (Cai et al. 2004; Palmstrom 2005; Kim et al. 2007; Macciotta and Derek 2015). Potential failure volumes can also be estimated for simulation purposes through analysis of the geometry of major discontinuities, as has been shown by many researchers. This work highlights the

importance of detailed and comprehensive structural and lithological models. Additionally, enhanced field data acquisition and modeling will require bridging our understanding of the multiple factors affecting rock avalanche runout through parametric physical models and thus should pay considerable attention to the role of discontinuities.

Furthermore, difficulties in representing discontinuity characteristics in laboratory experiments can be overcome by applying novel techniques, such as jointed analog blocks (Lin et al. 2020) or arrangement of bricks (Manzella and Labieuse 2009). In addition, physical experiments in laboratory or field environments are still insufficient to reveal the effects of discontinuities on rock avalanches. Although some physical experiments have studied the fragmentation of blocks with distinct discontinuities (Bowman et al. 2012; Lin et al. 2020), statistical information on the discontinuity of the failure mass is still absent. As mentioned above, characterizing complex discontinuities in the failure and sliding rock mass using quantitative parameters is also necessary for physical experiments. Moreover, comparison studies between small-scale physical experiments and realistic field cases of rock avalanches are recommended.

Concluding remarks

This paper presents a systematic and comprehensive review of the state of understanding of the role of discontinuities in the susceptibility of a rock slope to failure during the development of failure and the runout of rock avalanches.

As a precursory factor, discontinuities control the kinematical feasibility of rock slope failure and the rock mass strength. This, together with the local topography, defines the susceptibility of the rock slope to failure. In such a way, discontinuities define the spatial distribution of rock slope failures. During the development of failure, existing discontinuities will propagate and coalesce to increase the slope deformation, therefore decreasing the resistance against failure, and the kinematics of detachment evolve. During runout, the control of discontinuities on rock avalanches is primarily reflected by the propagation processes and the morphology characteristics of the deposits. Effective shear and fragmentation accompanied by heterogeneous stress and block distributions, which will make the propagation longer, are significantly controlled by preexisting discontinuities or weak lithological units and in turn define the mobility and characteristics of avalanche deposits. Efficient energy transfer in the finest fraction leads to longer runout and is also affected by microscopic discontinuities.

This paper further proposes some perspectives on further research. It is suggested to directly compare the characteristics of discontinuities in the source area and the runout of rock avalanches based on data collected from realistic field cases, and this comparison should be done when the other factors are similar. It is also suggested to explicitly and precisely represent discontinuities in back analyses and numerical and physical simulations, which will promote the understanding of the mechanism behind the role of discontinuities in the runout of rock avalanches, and novel techniques, such as laser scanning and photogrammetry, should be applied first to acquire precise discontinuity data.

It should be noted that the dynamics of rock avalanches are highly complex. A long-standing controversial issue will still remain with regard to how discontinuities control or affect the dynamics of rock avalanches. There will likely not be a straightforward

conclusion. The inherent geology might play a dominant role in determining their enhancing or weakening effect in the various stages of rock avalanches.

Acknowledgements

The comments from the editor and the anonymous reviewers were very helpful in improving the manuscript.

Funding

This study was supported by the Second Tibetan Plateau Scientific Expedition and Research (STEP) program (Grant NO. 2019QZKK0904), the National Natural Science Foundation of China (Grant NO. 42041006, 41927806, 41941019), and the National Key R&D Program of China (Grant NO. 2019YFC1520601).

Declarations

Conflict of interest The authors declare no competing interests.

References

- Aaron J, Hungr O (2016) Dynamic simulation of the motion of partially-coherent landslides. *Eng Geol* 205:1–11. <https://doi.org/10.1016/j.enggeo.2016.02.006>
- Abele G (1994) Large rockslides: their causes and movement on internal sliding planes. *Mt Res Dev* 14(4):315–320. <https://doi.org/10.2307/3673727>
- Bagnold RA (1954) Experiments on a gravity-free dispersion of large solid spheres in a Newtonian fluid under shear. *Proc R Soc Lond A* 225(1160):49–63. <https://doi.org/10.1098/rspa.1954.0186>
- Bao H, Zhai Y, Lan H, Zhang K, Qi Q, Yan C (2019) Distribution characteristics and controlling factors of vertical joint spacing in sand-mud interbedded strata. *J Struct Geol* 128:103886. <https://doi.org/10.1016/j.jsg.2019.103886>
- Bao H, Zhang G, Lan H, Yan C, Xu J, Xu W (2020) Geometrical heterogeneity of the joint roughness coefficient revealed by 3D laser scanning. *Eng Geol* 265:105415. <https://doi.org/10.1016/j.enggeo.2019.105415>
- Barth N (2014) The Cascade rock avalanche: implications of a very large Alpine Fault-triggered failure. *New Zealand Landslides* 11(3):327–341. <https://doi.org/10.1007/s10346-013-0389-1>
- Beguería S, Van Asch TW, Malet J-P, Gröndahl S (2009) A GIS-based numerical model for simulating the kinematics of mud and debris flows over complex terrain. *Nat Hazards Earth Syst Sci* 9:1897–1909. <https://doi.org/10.5194/nhess-9-1897-2009>
- Benko B, Stead D (1998) The Frank slide: a reexamination of the failure mechanism. *Can Geotech J* 35(2):299–311. <https://doi.org/10.1139/t98-005>
- Boon CW, Houlsby G, Utili S (2015) A new rock slicing method based on linear programming. *Comput Geotech* 65:12–29. <https://doi.org/10.1016/j.compgeo.2014.11.007>
- Bowman E, Take W, Rait K, Hann C (2012) Physical models of rock avalanche spreading behaviour with dynamic fragmentation. *Can Geotech J* 49(4):460–476. <https://doi.org/10.1139/t2012-007>
- Brideau M-A, Stead D, Kinakin D, Fecova K (2005) Influence of tectonic structures on the Hope Slide, British Columbia, Canada. *Eng Geol* 80(3–4):242–259. <https://doi.org/10.1016/j.enggeo.2005.05.004>
- Cagnoli B, Romano G (2012) Effects of flow volume and grain size on mobility of dry granular flows of angular rock fragments: a functional relationship of scaling parameters. *J Geophys Res Solid Earth* 117:B02207. <https://doi.org/10.1029/2011JB008926>
- Cai M, Kaiser P, Uno H, Tasaka Y, Minami M (2004) Estimation of rock mass deformation modulus and strength of jointed hard rock masses using the GSI system. *Int J Rock Mech Min Sci* 41(1):3–19. [https://doi.org/10.1016/S1365-1609\(03\)00025-X](https://doi.org/10.1016/S1365-1609(03)00025-X)
- Campbell CS, Cleary PW, Hopkins M (1995) Large-scale landslide simulations: global deformation, velocities and basal friction. *J Geophys Res Solid Earth* 100(B5):8267–8283. <https://doi.org/10.1029/94jbo0937>
- Catane SG, Cabria HB, Zarco MAH, Saturay RM, Mirasol-Robert AA (2008) The 17 February 2006 Guinsaugon rock slide-debris avalanche, Southern Leyte, Philippines: deposit characteristics and failure mechanism. *Bull Eng Geol Env* 67(3):305. <https://doi.org/10.1007/s10064-008-0120-y>
- Charrière M, Humair F, Froese C, Jaboyedoff M, Pedrazzini A, Longchamp C (2016) From the source area to the deposit: Collapse, fragmentation, and propagation of the Frank Slide. *Geol Soc Am Bull* 128(1–2):332–351. <https://doi.org/10.1130/B31243.1>
- Clavero J, Sparks R, Huppert H, Dade W (2002) Geological constraints on the emplacement mechanism of the Parinacota debris avalanche, northern Chile. *Bull Volcanol* 64(1):40–54. <https://doi.org/10.1007/s00445-001-0183-0>
- Corominas J (1996) The angle of reach as a mobility index for small and large landslides. *Can Geotech J* 33(2):260–271. <https://doi.org/10.1139/t96-005>
- Crosta G, Frattini P, Fusi N, Sosio R (2006) Formation, characterization and modelling of the 1987 Val Pola rock-avalanche dam (Italy). *Italian J Eng Geol Envir Special Issue* 1:145–150. https://doi.org/10.1007/978-3-642-04764-0_12
- Crosta G, Di Prisco C, Frattini P, Frigerio G, Castellanza R, Agliardi F (2014) Chasing a complete understanding of the triggering mechanisms of a large rapidly evolving rockslide. *Landslides* 11(5):747–764. <https://doi.org/10.1007/s10346-013-0433-1>
- Crosta GB, Frattini P, Fusi N (2007) Fragmentation in the Val Pola rock avalanche, Italian alps. *J Geophys Res Earth Surf* 112:F01006. <https://doi.org/10.1029/2005jf000455>
- Cruden D, Krahn J (1973) A reexamination of the geology of the Frank Slide. *Can Geotech J* 10(4):581–591. <https://doi.org/10.1139/t73-054>
- Cundall PA, Strack OD (1979) A discrete numerical model for granular assemblies. *Geotechnique* 29(1):47–65. <https://doi.org/10.1680/geot.1979.29.1.47>
- Dai F, Xu C, Yao X, Xu L, Tu X, Gong Q (2011) Spatial distribution of landslides triggered by the 2008 Ms 8.0 Wenchuan earthquake, China. *J Asian Earth Sci* 40(4):883–895. <https://doi.org/10.1016/j.jseaes.2010.04.010>
- Davies T, McSaveney M (2009) The role of rock fragmentation in the motion of large landslides. *Eng Geol* 109(1–2):67–79. <https://doi.org/10.1016/j.enggeo.2008.11.004>
- Davies TR, Reznichenko NV, McSaveney MJ (2020) Energy budget for a rock avalanche: fate of fracture-surface energy. *Landslides* 17(1):3–13. <https://doi.org/10.1007/s10346-019-01224-5>
- Do TN, Wu J-H (2020) Simulating a mining-triggered rock avalanche using DDA: a case study in Nattai North. *Australia Eng Geol* 264:105386. <https://doi.org/10.1016/j.enggeo.2019.105386-y>
- Donati D, Stead D, Elmo D, Onsel E (2020) New techniques for characterising damage in rock slopes: implications for engineered slopes and open pit mines. In: Dight PM (ed) *Slope Stability 2020: Proceedings of the 2020 International Symposium on Slope Stability in Open Pit Mining and Civil Engineering*. Australian Centre for Geomechanics, Perth, pp 129–144. https://doi.org/10.36487/ACG_repo/2025_03
- Dubovskoi A, Pernik L, Strom A (2008) Experimental simulation of rockslide fragmentation. *J Min Sci* 44(2):123–130. <https://doi.org/10.1007/s10913-008-0025-y>
- Dufresne A (2014) An overview of rock avalanche-substrate interactions. An overview of rock avalanche-substrate interactions. In:

- Sassa K, Canuti P, Yin Y (eds) *Landslide science for a safer geoenvironment*. Springer, Cham, pp 345–349. https://doi.org/10.1007/978-3-319-04999-1_49
- Dufresne A, Bösmeier A, Prager C (2016) Sedimentology of rock avalanche deposits—case study and review. *Earth Sci Rev* 163:234–259. <https://doi.org/10.1016/j.earscirev.2016.10.002>
- Dufresne A, Dunning S (2017) Process dependence of grain size distributions in rock avalanche deposits. *Landslides* 14(5):1555–1563. <https://doi.org/10.1007/s10346-017-0806-y>
- Dunning S (2006) The grain size distribution of rock-avalanche deposits in valley-confined settings. *Italian J Eng Geol Environ* 1:117–121. <https://doi.org/10.4408/IJEGE.2006-01.S-15>
- Dunning SA, Armitage P (2011) The grain-size distribution of rock-avalanche deposits: implications for natural dam stability. In: Evans S, Hermanns R, Strom A, Scarascia-Mugnozza G (eds) *Natural and artificial rockslide dams, lecture notes in earth sciences*, vol 133. Springer, Berlin, Heidelberg, pp 479–498. https://doi.org/10.1007/978-3-642-04764-0_19
- Fan X et al (2017) Failure mechanism and kinematics of the deadly June 24th 2017 Xinmo landslide, Maoxian, Sichuan, China. *Landslides* 14(6):2129–2146. <https://doi.org/10.1007/s10346-017-0907-7>
- Guo D, Hamada M, He C, Wang Y, Zou Y (2014) An empirical model for landslide travel distance prediction in Wenchuan earthquake area. *Landslides* 11(2):281–291. <https://doi.org/10.1007/s10346-013-0444-y>
- Haug ØT, Rosenau M, Rudolf M, Leever K, Oncken O (2021) Short communication: Runout of rock avalanches limited by basal friction but controlled by fragmentation. *Earth Surf Dynam* 9:665–672. <https://doi.org/10.5194/esurf-9-665-2021>
- Hewitt K (1999) Quaternary moraines vs catastrophic rock avalanches in the Karakoram Himalaya, northern Pakistan. *Quatern Res* 51(3):220–237. <https://doi.org/10.1006/qres.1999.2033>
- Hsu KJ (1975) Catastrophic debris streams (sturzstroms) generated by rockfalls. *Geol Soc Am Bull* 86(1):129–140. [https://doi.org/10.1130/0016-7606\(1975\)86<129:CDSSGB>2.0.CO;2](https://doi.org/10.1130/0016-7606(1975)86<129:CDSSGB>2.0.CO;2)
- Hungr O, Leroueil S, Picarelli L (2014) The Varnes classification of landslide types, an update. *Landslides* 11(2):167–194. <https://doi.org/10.1007/s10346-013-0436-y>
- Hutter K, Koch T, Plüß C, Savage S (1995) The dynamics of avalanches of granular materials from initiation to runout. Part II. Experiments. *Acta Mech* 109(1–4):127–165. <https://doi.org/10.1007/BF01176820>
- Iverson RM, Ouyang C (2015) Entrainment of bed material by Earth-surface mass flows: Review and reformulation of depth-integrated theory. *Rev Geophys* 53(1):27–58. <https://doi.org/10.1002/2013RG000447>
- Jaboyedoff M, Metzger R, Oppikofer T, Couture R, Derron M, Locat J, Turmel D (2007) New insight techniques to analyze rock-slope relief using DEM and 3D-imaging cloud points: COLTOP-3D software. In: *Rock mechanics: meeting society's challenges and demands*, pp 61–68. <https://doi.org/10.1201/NOE0415444019-c8>
- Johnson BC, Campbell CS, Melosh HJ (2016) The reduction of friction in long runout landslides as an emergent phenomenon. *J Geophys Res Earth Surf* 121(5):881–889. <https://doi.org/10.1002/2015jf003751>
- Keefer DK (1984) Rock avalanches caused by earthquakes: source characteristics. *Science* 223(4642):1288–1290. <https://doi.org/10.1126/science.223.4642.1288>
- Kent P (1966) The transport mechanism in catastrophic rock falls. *J Geol* 74(1):79–83. <https://doi.org/10.1086/627142>
- Kim B, Cai M, Kaiser P, Yang H (2007) Estimation of block sizes for rock masses with non-persistent joints. *Rock Mech Rock Eng* 40(2):169. <https://doi.org/10.1007/s00603-006-0093-8>
- Kim Y-S, Peacock DC, Sanderson DJ (2004) Fault damage zones. *J Struct Geol* 26(3):503–517. <https://doi.org/10.1016/j.jsg.2003.08.002>
- Lan H, Hu R, Yue Z, Lee C, Wang S (2003) Engineering and geological characteristics of granite weathering profiles in South China. *J Asian Earth Sci* 21(4):353–364. [https://doi.org/10.1016/S1367-9120\(02\)00020-2](https://doi.org/10.1016/S1367-9120(02)00020-2)
- Lan H, Zhou C, Wang L, Zhang H, Li R (2004) Landslide hazard spatial analysis and prediction using GIS in the Xiaojiang watershed, Yunnan, China. *Eng Geol* 76(1–2):109–128. <https://doi.org/10.1016/j.enggeo.2004.06.009>
- Lan H, Lee C, Zhou C, Martin C (2005) Dynamic characteristics analysis of shallow landslides in response to rainfall event using GIS. *Environ Geol* 47(2):254–267. <https://doi.org/10.1007/s00254-004-1151-8>
- Lan H, Martin CD, Hu B (2010) Effect of heterogeneity of brittle rock on micromechanical extensile behavior during compression loading. *J Geophys Res Solid Earth* 115:B01202. <https://doi.org/10.1029/2009JB006496>
- Lan H, Chen J, Macciotta R (2019) Universal confined tensile strength of intact rock. *Sci Rep* 9:6170. <https://doi.org/10.1038/s41598-019-42698-6>
- Legros F (2002) The mobility of long-runout landslides. *Eng Geol* 63(3–4):301–331. [https://doi.org/10.1016/S0013-7952\(01\)00090-4](https://doi.org/10.1016/S0013-7952(01)00090-4)
- Leroueil S (2001) Natural slopes and cuts: movement and failure mechanisms. *Géotechnique* 51(3):197–243. <https://doi.org/10.1680/geot.2001.51.3.197>
- Li L, Lan H, Wu Y (2014) The volume-to-surface-area ratio constrains the rollover of the power law distribution for landslide size. *Eur Phys J Plus* 129(5):89. <https://doi.org/10.1140/epjp/i2014-14089-y>
- Li L, Lan H, Wu Y (2016) How sample size can effect landslide size distribution. *Geoenviron Disasters* 3(1):18. <https://doi.org/10.1186/s40677-016-0052-y>
- Li L, Lan H, Guo C, Zhang Y, Li Q, Wu Y (2017) A modified frequency ratio method for landslide susceptibility assessment. *Landslides* 14(2):727–741. <https://doi.org/10.1007/s10346-016-0771-x>
- Lin Q, Cheng Q, Xie Y, Zhang F, Li K, Wang Y, Zhou Y (2021) Simulation of the fragmentation and propagation of jointed rock masses in rockslides: DEM modeling and physical experimental verification. *Landslides* 18(3):993–1009. <https://doi.org/10.1007/s10346-020-01542-z>
- Lin Q, Cheng Q, Li K, Xie Y, Wang Y (2020) Contributions of rock mass structure to the emplacement of fragmenting rockfalls and rockslides: insights from laboratory experiments. *J Geophys Res Solid Earth* 125(4):e2019JB019296. <https://doi.org/10.1029/2019JB019296>
- Locat P, Couture R, Locat J, Leroueil S (2003) Assessment of the fragmentation energy in rock avalanches. In: *3rd Canadian Conference on Geotechnique and Geohazards*, pp 261–268
- Locat P, Couture R, Leroueil S, Locat J, Jaboyedoff M (2006) Fragmentation energy in rock avalanches. *Can Geotech J* 43(8):830–851. <https://doi.org/10.1139/t06-045>
- Lucas A, Mangeney A, Ampuero JP (2014) Frictional velocity-weakening in landslides on Earth and on other planetary bodies. *Nat Commun* 5:3417. <https://doi.org/10.1038/ncomms4417>
- Macciotta R, Derek MC (2015) Remote structural mapping and discrete fracture networks to calculate rock fall volumes at Tornado Mountain, British Columbia. In: *49th US Rock Mechanics/Geomechanics Symposium*. American Rock Mechanics Association
- Manzella I, Labiouse V (2009) Flow experiments with gravel and blocks at small scale to investigate parameters and mechanisms involved in rock avalanches. *Eng Geol* 109(1–2):146–158. <https://doi.org/10.1016/j.enggeo.2008.11.006>
- Margielewski W (2006) Structural control and types of movements of rock mass in anisotropic rocks: case studies in the Polish Flysch Carpathians. *Geomorphology* 77(1–2):47–68. <https://doi.org/10.1016/j.geomorph.2006.01.003>
- McDougall S (2017) 2014 Canadian Geotechnical Colloquium: landslide runout analysis—current practice and challenges. *Can Geotech J* 54(5):605–620. <https://doi.org/10.1139/cgj-2016-0104>
- Mergili M, Schratz K, Ostermann A, Fellin W (2012) Physically-based modelling of granular flows with Open Source GIS. *Nat Hazard* 12(1):187. <https://doi.org/10.5194/nhess-12-187-2012>
- Mergili M, Fischer J-T, Krenn J, Pudasaini SP (2017) r. avaflow v1, an advanced open-source computational framework for the propa-

- gation and interaction of two-phase mass flows. *Geosci Model Dev* 10(2):553–569. <https://doi.org/10.5194/gmd-10-553-2017>
- Mitchell A, McDougall S, Nolde N, Brideau M-A, Whittall J, Aaron J (2020) Rock avalanche runout prediction using stochastic analysis of a regional dataset. *Landslides* 17:777–792. <https://doi.org/10.1007/s10346-019-01331-3>
- Nicoletti PG, Sorriso-Valvo M (1991) Geomorphic controls of the shape and mobility of rock avalanches. *Geol Soc Am Bull* 103(10):1365–1373. [https://doi.org/10.1130/0016-7606\(1991\)103<1365:GCOTSA>2.3.CO;2](https://doi.org/10.1130/0016-7606(1991)103<1365:GCOTSA>2.3.CO;2)
- Oppikofer T, Jaboyedoff M, Keusen H-R (2008) Collapse at the eastern Eiger flank in the Swiss Alps. *Nat Geosci* 1(8):531–535. <https://doi.org/10.1038/ngeo258>
- Ouyang CJ, Zhao W, He SM, Wang DP, Zhou S, An HC, Wang ZW, Cheng DX (2017) Numerical modeling and dynamic analysis of the 2017 Xinmo landslide in Maoxian County, China. *J Mt Sci* 14(9):1701–1711. <https://doi.org/10.1007/s11629-017-4613-7>
- Paguican E, Van Wyk de Vries B, Lagmay AM (2014) Hummocks: how they form and how they evolve in rockslide-debris avalanches. *Landslides* 11(1):67–80. <https://doi.org/10.1007/s10346-012-0368-y>
- Palmstrom A (2005) Measurements of and correlations between block size and rock quality designation (RQD). *Tunn Undergr Space Technol* 20(4):362–377. <https://doi.org/10.1016/j.tust.2005.01.005>
- Palmström A (2001) Measurement and characterization of rock mass jointing. In: Sharma VM, Saxena KR (eds) *In situ characterization of rocks*. Balkema, Tokyo, pp 49–97
- Pastor M, Crosta G (2012) Landslide runout: review of analytical/empirical models for subaerial slides, submarine slides and snow avalanche. Numerical modelling. Software tools, material models, validation and benchmarking for selected case studies. Deliverable D1.7 for SafeLand project
- Pedrazzini A, Froese C, Jaboyedoff M, Hungr O, Humair F (2012) Combining digital elevation model analysis and run-out modeling to characterize hazard posed by a potentially unstable rock slope at Turtle Mountain, Alberta, Canada. *Eng Geol* 128:76–94. <https://doi.org/10.1016/j.enggeo.2011.03.015>
- Pedrazzini A, Jaboyedoff M, Loye A, Derron M-H (2013) From deep seated slope deformation to rock avalanche: destabilization and transportation models of the Sierre landslide (Switzerland). *Tectonophysics* 605:149–168. <https://doi.org/10.1016/j.tecto.2013.04.016>
- Petley DN (2013) Characterizing giant landslides. *Science* 339(6126):1395–1396. <https://doi.org/10.1126/science.1236165>
- Pollet N, Schneider J-L (2004) Dynamic disintegration processes accompanying transport of the Holocene Flims sturzstrom (Swiss Alps). *Earth Planet Sci Lett* 221(1–4):433–448. [https://doi.org/10.1016/S0012-821X\(04\)00071-8](https://doi.org/10.1016/S0012-821X(04)00071-8)
- Qi S, Xu Q, Zhang B, Zhou Y, Lan H, Li L (2011) Source characteristics of long runout rock avalanches triggered by the 2008 Wenchuan earthquake, China. *J Asia Earth Sci* 40(4):896–906. <https://doi.org/10.1016/j.jseaes.2010.05.010>
- Sassa K, Nagai O, Solidum R, Yamazaki Y, Ohta H (2010) An integrated model simulating the initiation and motion of earthquake and rain induced rapid landslides and its application to the 2006 Leyte landslide. *Landslides* 7(3):219–236. <https://doi.org/10.1007/s10346-010-0230-z>
- Scaringi G, Fan XM, Xu Q, Liu C, Ouyang CJ, Domènech G, Yang F, Dai LX (2018) Some considerations on the use of numerical methods to simulate past landslides and possible new failures: the case of the recent Xinmo landslide (Sichuan, China). *Landslides* 15(7):1359–1375. <https://doi.org/10.1007/s10346-018-0953-9>
- Schilirò L, Esposito C, De Blasio F, Mugnozsa GS (2019) Sediment texture in rock avalanche deposits: insights from field and experimental observations. *Landslides* 16(9):1629–1643. <https://doi.org/10.1007/s10346-019-01210-x>
- Schramm J-M, Weidinger JT, Ibetsberger H (1998) Petrologic and structural controls on geomorphology of prehistoric Tsergo Ri slope failure, Langtang Himal, Nepal. *Geomorphology* 26(1–3):107–121. [https://doi.org/10.1016/S0169-555X\(98\)00053-1](https://doi.org/10.1016/S0169-555X(98)00053-1)
- Sejmonsbergen A, Woning M, Verhoef P, De Graaff L (2005) The failure mechanism of a Late Glacial sturzstrom in the subalpine Molasse (Leckner Valley, Vorarlberg, Austria). *Geomorphology* 66(1–4):277–286. <https://doi.org/10.1016/j.geomorph.2004.09.016>
- Severin J, Eberhardt E, Leoni L, Fortin S (2014) Development and application of a pseudo-3D pit slope displacement map derived from ground-based radar. *Eng Geol* 181:202–211. <https://doi.org/10.1016/j.enggeo.2014.07.016>
- Shea T, van Wyk de Vries B (2008) Structural analysis and analogue modeling of the kinematics and dynamics of rockslide avalanches. *Geosphere* 4(4):657–686. <https://doi.org/10.1130/GES001311>
- Sosio R, Crosta GB, Hungr O (2008) Complete dynamic modeling calibration for the Thurwieser rock avalanche (Italian Central Alps). *Eng Geol* 100(1–2):11–26. <https://doi.org/10.1016/j.enggeo.2008.02.012>
- Strom A (2006) Morphology and internal structure of rockslides and rock avalanches: grounds and constraints for their modelling. In: Evans SG, Mugnozsa GS, Strom A, Hermanns RL (eds) *Landslides from massive rock slope failure*, NATO Science Series, vol 49. Springer, Dordrecht, pp 305–326. https://doi.org/10.1007/978-1-4020-4037-5_17
- Strom A (2015) Peculiarities of large landslides' morphology and internal structure: constraints of their motion modelling. In: Lollino G, Giordan D, Crosta GB, Corominas J, Azzam R, Wasowski J, Sciarra N (eds) *Engineering geology for society and territory*, vol 2. Springer, Cham, pp 1691–1694. https://doi.org/10.1007/978-3-319-09057-3_300
- Strom A, Abdrakhmatov K (2018) Rockslides and rock avalanches of Central Asia: distribution, morphology, and internal structure. Elsevier. <https://doi.org/10.1016/C2014-0-02190-9>
- Strom A, Li L, Lan H (2019) Rock avalanche mobility: optimal characterization and the effects of confinement. *Landslides* 16(8):1437–1452. <https://doi.org/10.1007/s10346-019-01181-z>
- Strom A (2021) Rock avalanches: basic characteristics and classification criteria. In: Vilímek V, Wang F, Strom A, Sassa K, Bobrowsky PT, Takara K (eds) *Understanding and reducing landslide disaster risk*, WLF 2020, ICL contribution to landslide disaster risk reduction. Springer, Cham, pp 3–23. https://doi.org/10.1007/978-3-030-60319-9_1
- Strom AL, Korup O (2006) Extremely large rockslides and rock avalanches in the Tien Shan Mountains, Kyrgyzstan. *Landslides* 3(2):125–136. <https://doi.org/10.1007/s10346-005-0027-7>
- Sun J, Wang X, Liu H, Yuan H (2021) Effects of the attitude of dominant joints on the mobility of translational landslides. *Landslides* 18:2483–2498. <https://doi.org/10.1007/s10346-021-01668-8>
- Taboada A, Estrada N (2009) Rock-and-soil avalanches: theory and simulation. *J Geophys Res Earth Surf* 114:F03004. <https://doi.org/10.1029/2008JF001072>
- Thompson N, Bennett MR, Petford N (2010) Development of characteristic volcanic debris avalanche deposit structures: new insight from distinct element simulations. *J Volcanol Geoth Res* 192(3–4):191–200. <https://doi.org/10.1016/j.jvolgeores.2010.02.021>
- Vick LM, Bergh SG, Höpfl S, Percival J, Daines EB (2020a) The role of lithological weakness zones in rockslides in northern Norway. In: *ISRM International Symposium - EUROCK 2020*
- Vick LM, Böhme M, Rouyet L, Bergh SG, Corner GD, Lauknes TR (2020b) Structurally controlled rock slope deformation in northern Norway. *Landslides* 17(8):1745–1776. <https://doi.org/10.1007/s10346-020-01421-7>
- Wang J, Zhang Y, Chen Y, Wang Q, Xiang C, Fu H, Wang P, Zhao J, Zhao L (2021) Back-analysis of Donghekou landslide using improved DDA considering joint roughness degradation. *Landslides* 18(5):1925–1935. <https://doi.org/10.1007/s10346-020-01586-1>

- Wang S, Xu W, Shi C, Chen H (2017) Run-out prediction and failure mechanism analysis of the Zhenggang deposit in southwestern China. *Landslides* 14(2):719–726. <https://doi.org/10.1007/s10346-016-0770-y>
- Wang YF, Cheng QG, Lin QW, Li K, Yang HF (2018) Insights into the kinematics and dynamics of the Luanshibao rock avalanche (Tibetan Plateau, China) based on its complex surface landforms. *Geomorphology* 317:170–183. <https://doi.org/10.1016/j.geomorph.2018.05.025>
- Wang YF, Cheng QG, Shi AW, Yuan YQ, Yin BM, Qiu YH (2019) Sedimentary deformation structures in the Nyixoi Chongco rock avalanche: implications on rock avalanche transport mechanisms. *Landslides* 16(3):523–532. <https://doi.org/10.1007/s10346-018-1117-7>
- Wang YF, Cheng QG, Yuan YQ, Wang J, Qiu YH, Yin BM, Shi AW, Guo ZW (2020) Emplacement mechanisms of the Tagarma rock avalanche on the Pamir-western Himalayan syntaxis of the Tibetan Plateau, China. *Landslides* 17(3):527–542. <https://doi.org/10.1007/s10346-019-01298-1>
- Weidinger JT, Schramm J-M, Surenian R (1996) On preparatory causal factors, initiating the prehistoric Tsergo Ri landslide (Langthang Himal, Nepal). *Tectonophysics* 260(1–3):95–107. [https://doi.org/10.1016/0040-1951\(96\)00078-9](https://doi.org/10.1016/0040-1951(96)00078-9)
- Weidinger JT (2006) Predesign, failure and displacement mechanisms of large rockslides in the Annapurna Himalayas, Nepal. *Eng Geol* 83(1–3):201–216. <https://doi.org/10.1016/j.enggeo.2005.06.032>
- Weidinger JT, Korup O, Munack H, Altenberger U, Dunning SA, Tippelt G, Lottermoser W (2014) Giant rockslides from the inside. *Earth Planet Sci Lett* 389:62–73. <https://doi.org/10.1016/j.epsl.2013.12.017>
- Wu Y, Lan H (2019) Landslide analyst—a landslide propagation model considering block size heterogeneity. *Landslides* 16(6):1107–1120. <https://doi.org/10.1007/s10346-019-01154-2>
- Wu Y, Lan H (2020) Debris flow analyst (DA): a debris flow model considering kinematic uncertainties and using a GIS platform. *Eng Geol* 279:105–877. <https://doi.org/10.1016/j.enggeo.2020.105877>
- Xu Q, Zhang S, Li W (2011) Spatial distribution of large-scale landslides induced by the 5.12 Wenchuan earthquake. *J Mt Sci* 8(2):246. <https://doi.org/10.1007/s11629-011-2105-8>
- Xu Q, Shang Y, van Asch T, Wang S, Zhang Z, Dong X (2012) Observations from the large, rapid Yigong rock slide–debris avalanche, southeast Tibet. *Can Geotech J* 49(5):589–606. <https://doi.org/10.1139/t2012-021>
- Yin Y, Wang F, Sun P (2009) Landslide hazards triggered by the 2008 Wenchuan earthquake, Sichuan, China. *Landslides* 6(2):139–152. <https://doi.org/10.1007/s10346-009-0148-5>
- Yin Y, Sun P, Zhang M, Li B (2011) Mechanism on apparent dip sliding of oblique inclined bedding rockslide at Jiweishan, Chongqing, China. *Landslides* 8(1):49–65. <https://doi.org/10.1007/s10346-010-0237-5>
- Zhan W, Fan X, Huang R, Pei X, Xu Q, Li W (2017) Empirical prediction for travel distance of channelized rock avalanches in the Wenchuan earthquake area. *Nat Hazards Earth Syst Sci* 17(6):833–844. <https://doi.org/10.5194/nhess-17-833-2017>
- Zhang H, Liu SQ, Wang W, Zheng L, Zhang YB, Wu YQ, Han Z, Li YG, Chen GQ (2018a) A new DDA model for kinematic analyses of rockslides on complex 3-D terrain. *Bull Eng Geol Env* 77(2):555–571. <https://doi.org/10.1007/s10064-016-0971-6>
- Zhang M, Yin Y, McSaveney M (2016) Dynamics of the 2008 earthquake-triggered Wenjiagou Creek rock avalanche, Qingping, Sichuan, China. *Eng Geol* 200:75–87. <https://doi.org/10.1016/j.enggeo.2015.12.008>
- Zhang M, McSaveney M (2017) Rock avalanche deposits store quantitative evidence on internal shear during runoff. *Geophys Res Lett* 44(17):8814–8821. <https://doi.org/10.1002/2017GL073774>
- Zhang M, McSaveney M, Shao H, Zhang C (2018b) The 2009 Jiweishan rock avalanche, Wulong, China: precursor conditions and factors leading to failure. *Eng Geol* 233:225–230. <https://doi.org/10.1016/j.enggeo.2017.12.010>
- Zhang M, Wu L, Zhang J, Li L (2019) The 2009 Jiweishan rock avalanche, Wulong, China: deposit characteristics and implications for its fragmentation. *Landslides* 16(5):893–906. <https://doi.org/10.1007/s10346-019-01142-6>
- Zhao T, Utili S, Crosta G (2016) Rockslide and impulse wave modelling in the Vajont reservoir by DEM-CFD analyses. *Rock Mech Rock Eng* 49(6):2437–2456. <https://doi.org/10.1007/s00603-015-0731-0>
- Zhao T, Crosta GB, Utili S, De Blasio FV (2017) Investigation of rock fragmentation during rockfalls and rock avalanches via 3-D discrete element analyses. *J Geophys Res Earth Surf* 122(3):678–695. <https://doi.org/10.1002/2016JF004060>
- Zhao T, Crosta GB, Dattola G, Utili S (2018) Dynamic fragmentation of jointed rock blocks during rockslide-avalanches: Insights from discrete element analyses. *J Geophys Res Solid Earth* 123(4):3250–3269. <https://doi.org/10.1002/2017JB015210>
- Zhou J-w, Cui P, Hao M-h (2016) Comprehensive analyses of the initiation and entrainment processes of the 2000 Yigong catastrophic landslide in Tibet, China. *Landslides* 13(1):39–54. <https://doi.org/10.1007/s10346-014-0553-2>

Hengxing Lan (✉) · Yixing Zhang · Langping Li (✉) · Yuming Wu

State Key Laboratory of Resources and Environmental Information System, Institute of Geographic Sciences and Natural Resources Research, Chinese Academy of Sciences, Beijing 100101, China

Hengxing Lan

Email: lanhx@lreis.ac.cn

Langping Li

Email: lilp@lreis.ac.cn

Hengxing Lan · Jianbing Peng

School of Geological Engineering and Geomatics, Chang'an University, Xi'an 710064, China

Renato Macciotta

Department of Civil and Environmental Engineering, University of Alberta, Edmonton, AB T6G 1H9, Canada

Han Bao

School of Highway, Chang'an University, Xi'an 710064, China